Near-fault Ground Displacement for Seismic Design of Bridge Structures

S.L. Wu [(1)], B. Charatpangoon[(2)], J. Kiyono [(3)], Y. Maeda [(4)], T. Nakatani [(5)],S.Y. Li[(6)]

[(1)] *Doctoral student, Dept. of Urban Management., Kyoto University, E-mail:wu.shuanglan.73v@st.kyoto-u.ac.jp*
[(2)] *Lecturer, Department of Civil Engineering, Faculty of Engineering, Chiang Mai University, E-mail: bhuddarak.c@cmu.ac.th*
[(3)] *Professor, Graduate School of Global Environmental Studies, Kyoto University, E-mail: kiyono.junji.5x@kyoto-u.ac.jp*
[(4)] *Alliance Professor of Kyushu University, Doyu Daichi Company Limited, E-mail: y.maeda@cdaichi.co.jp*
[(5)] *Doyu Daichi Company Limited, E-mail: t.nakatani@cdaichi.co.jp*
[(6)] *Doyu Daichi Company Limited, E-mail: s.li@cdaichi.co.jp*

Abstract

When structures located near or across the faults, the effects of ground displacement as well as velocity and acceleration are crucial factors, since the faults produce both step-like static deformation and dynamic pulse-like ground motions. Moreover, the fling-containing time histories are necessary for the seismic analysis and design of bridge structures. As has been observed before, the static offsets can reach from several centimeters to 10 meters (e.g., the Chi-Chi earthquake), and strong ground motion velocity pulses may exceed 100 cm/s. Until now, as there is no concrete synthesis method of design ground displacement, numerical simulation of strong ground motions, emphases on input ground displacement in this study, for such near-fault conditions are very necessary. This paper proposes a hybrid method based on coupling of the stochastic Green's function method and theoretical Green's function method. This hybrid method considers both dynamic and static terms. For illustrating the application of this hybrid method, a simulation of one dip-slip fault model was conducted. The results well featured the near-fault ground motions of dynamic displacement with the fling-step. Furthermore, the procedure for seismic design of bridge structures located close or cross fault under multi-input of velocities and displacements, which are simulated by this proposed method is briefly introduced, and a simple 4-span bridge structure across a reverse surface fault was analyzed. The calculation results showed that the synchronized time-histories inputs lead to significant differences in the dynamic response of bridge, which provide a useful reference for the design guidelines for such near-fault bridge engineering.

Keywords: near-fault ground motion, numerical simulation, static terms, dynamic terms, seismic design of bridge

1. Introduction

A number of significant inland earthquakes tragically occurred successively, such as the 1994 Northridge earthquake (Mw 6.7), the 1995 Kobe earthquake (Mw 6.9), the 1999 Izmit, Turkey, the 1999 Chi-Chi earthquake (Mw 7.6-7.7), the 2015 Nepal Earthquake (Mw 7.8), and the 2016 Kumamoto earthquake (Mw 7.0). These seismic events had devastating effects on urban infrastructures. If the inland fault is located or runs close to the structures, (e.g., the situation shown in Fig. 1, the bridge across the fault), its ground displacement can be detrimental especially for spatially extended and flexible structures, such as long-span bridges, embankment, highways, etc. Thus, the characterization, causative parameterization, analytical modeling, and numerical simulation methods of near-fault seismic ground motions, as well as theirs effects on the responses of engineering structures, are extremely essential and needed to be clarified.

Up to date, even though there are extensive researches focusing on the near-fault ground motions: Mavroeidis and Papageorgiou proposed an analytical model with four parameters (the pulse duration, the pulse amplitude, the nubmer and phase of half cycles) to describe the entire set of velocity pulses generated due to forward directivity or permanent translation effects [1]; based on the stiffness matrix method, Wang made an anal6ysis on near-fault ground motions in details [2]; based on the double impulse [3] and a series of researches [4][5], Kojima and Takewaki proposed a new approach which is intended to simplify the fling-step and forward-directivity input of typical near-fault ground motions by a double impulse and a triple impulse, separately; also despite the seismograms recordings by broadband digital strong motion instruments have been appreciably improved, the importance of the effect of near-fault ground motion to the structure was underestimated, and a rational and simple seismic design philosophy for such structures has not been established yet. Here a simple synthesis hybrid method for simulating the near-fault strong ground motions is presented, and then by adoption of this proposed method, seismic response of a four-span bridge was conducted, using multi-input ground motions with permanent displacements as the Fig. 1 showing.

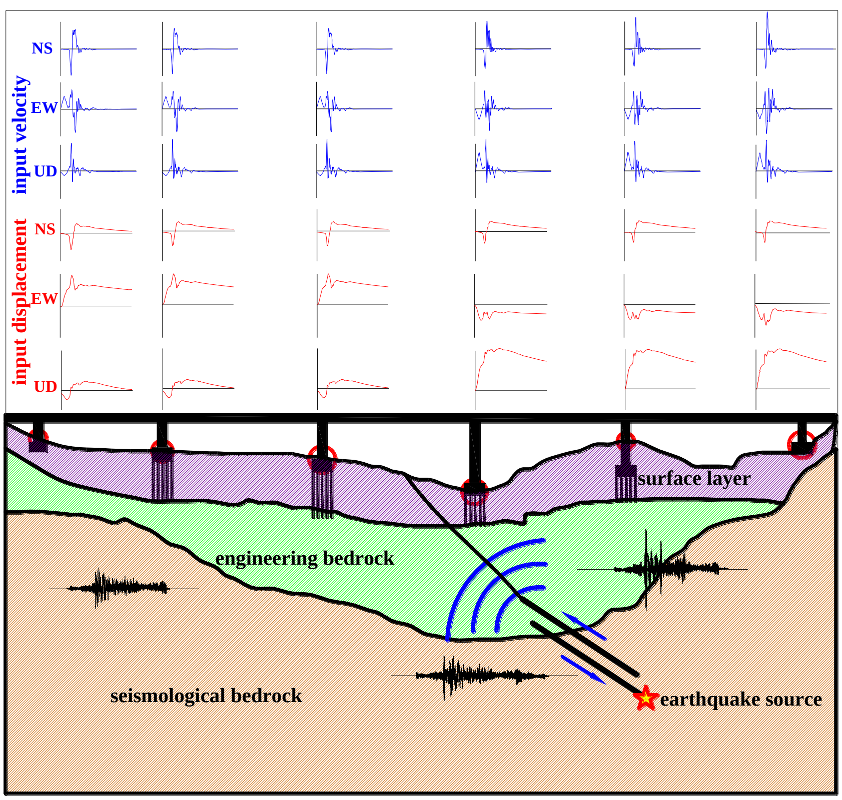

Fig.1 – multi-input ground motions for near-fault bridge structures

(a) en enchelon fissures

(b) reverse fault

Fig. 2 - Surface rupture of the 2016 Kumamoto earthquake

2. Methodology

As for the simulated time histories for near-fault ground motions, it is highly required that it must accurately incorporate the near-fault source radiation pattern, accounting for far- and near-field seismic radiation, and have the ability to characterize motions for a broad range of fault types (e.g., strike-slip, normal and reverse faulting), as well as variable slip and full kinematic description of the rupture process. We must be able to simulate the directivity effect as well as the sudden elastic rebound (sometimes referred to as fling) accurately. Thus, it needs to calculate motions very close to the fault; we here consider the fling-step effect and velocity pulses as important characteristics of near-fault ground motions.

2.1 Hybrid method

Firstly, the displacement due to a kinematical fault model can be expressed as the following equation (1) in the frequency domain:

$$U_k(\mathbf{Y},\omega)=\int_S T_{ik}(\mathbf{X},\mathbf{Y};\omega)D_i(\mathbf{X};\omega)dS \tag{1}$$

Where U_k is the *kth* component of displacement in Cartesian coordinate system at an observation point ***Y***, ***X*** is a source point on the fault plane, ω is the circular frequency; S is the fault plane, T_{ik} is the traction Green's function, and D_i is the *ith* component of the fault slip.

In order to simulate theoretical strong ground motions for near-faults, Hisada and Bielak [6] introduced an efficient method for carrying out integration of the representation theorem, which evaluates the fault integration of the dynamic and static terms, separately as the Eq. (2) shown,

$$U_k(\mathbf{Y},\omega)=\int_S\left\{T_{ik}^D(\mathbf{X},\mathbf{Y};\omega)-T_{ik}^S(\mathbf{X},\mathbf{Y})\right\}D_i(\mathbf{X};\omega)dS+\int_S T_{ik}^S(\mathbf{X},\mathbf{Y})D_i(\mathbf{X};\omega)dS \tag{2}$$

Where T_{ik}^D and T_{ik}^S are the dynamic and static traction Green's functions in layered half-space.

The theoretical Green's function for generation of dynamic motion lacks of general versatility although the method is very sophisticated, while since the statistical Green's function method is very popular, widely used, and successfully applied to structural designs. Therefore, we proposed a hybrid simulation method of modified statistical (dynamic) and theoretical (static) Green's function for synthesizing the near-fault ground displacement. Moreover, it is much faster when compared with some other simulation methods.

2.2 Modified statistic Green's function method

As observation point is close to the fault plane, the waveforms exhibit sharp peaks of short duration within the area which located close to the observation point [6]. Even if the distance to fault is very short, the dynamic ground motion can be calculated by superposing small element waveforms. Thus, in this paper, the modified statistical Green's function method [7][8] is adopted for calculating the dynamic terms.

The basic principle of original statistical Green's function method is as following: a large earthquake is composed of a series of small earthquakes; and stochastically calculated small earthquakes are properly selected as ground response caused by small areal sources, namely statistical Green's functions which are then overlaid by specified cracking ways to obtain the time-history curve of large earthquake. Both displacement spectra and acceleration spectra are introduced to determine the quantity of neutron source and stress drop ratio, which are compared with parameters obtained from the similarity of large earthquake and small earthquake for purpose of obtaining proper parameters of hypocenter, Eqs. (3) ~ (4) listed the main procedure of this method.

$$U(t)=\sum_{m=1}^{NL}\sum_{n=1}^{NW}\frac{r}{r_{mn}}\left[u(t-t_{mn})+\sum_{k=1}^{(ND-1)n'}\frac{1}{n'}u(t-t_{mn}-(k-1)\cdot\frac{\tau}{(ND-1)n'})\right] \tag{3}$$

$$t_{mn} = \frac{(r_{mn} - r_o)}{V_s} + \frac{\xi_{mn}}{V_R} \tag{4}$$

where, *U(t)*is the synthetic main-shock ground motion displacement, *u(t)* is observation small ground motion, *NL*, *NW* and *ND* are the ratios of the fault dimensions (the fault length and width) and slip values between large and small events; and t_{mn} is the delay time of point source *(m,n)* on the rupture surface, τ is the rise time of small earthquake, Vs and V_R stand for the S-wave velocity near the earthquake source and rupture velocity respectively. ξ_{mn} is the distance from the point *(m,n)* located on the fault plane to the starting point. And *n'* is an appropriate integer to weaken the artificial periodicity of *n*, and to adjust the interval of the tick to be the sampling rate. For other notations, the schematic diagram on superposition of small events are shown in Fig. 3.

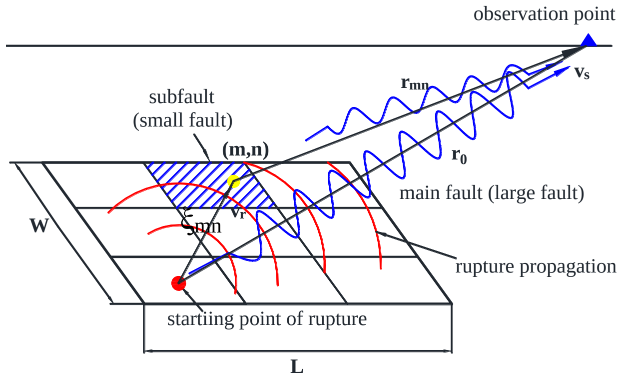

Fig. 3 - Schematic illustrations of statistical Green's Function method

As for the conventional statistical Green's function method just considers the far-field terms of S-wave, while as for the complete waveforms, especially the very near source observation sites, all the items, including the near-, intermediate-, and far-field items of P-waves and S-waves should be taken into considerations. The research [9] calculated the complete waveforms by using a finite-difference, and Onishi and Horike [10] improved the stochastic Green's functions by introducing the theoretical radiation coefficients of the P-, SV-, and SH-waves and a ray tracing technique in layered half-spaces. In this paper, based on the method proposed by Nozu [11], the complete waveforms, which introducing the near-field and intermediate-field terms, as well as the far-field P-waves are calculated in this proposed method.

2.3 Theoretical Green's function method

As the statistical Green's function method does not consider the static displacement because the stochastically calculated small earthquake does not contain permanent displacement, even if the observation point is located very close to the fault. For the purpose of obtaining the near-fault time history, the static terms, which means the second integral describes the attenuation of slip function in the right side of equation (1) due to the static traction of Green's functions, and the theoretical Green's functions are calculated by wavenumber integration method [12~15]. Thus, in this study, we only adopt the second terms of Eq. (2) and calculate the static displacement according to the Eq. (5) as following:

$$U_k(\mathbf{Y};\omega) = \int_S T_{ik}^S(\mathbf{X},\mathbf{Y}) D_i(\mathbf{X};\omega) dS \tag{5}$$

where $U_k(\mathbf{Y};\ \omega)$ is the static displacement, in this situation, $\omega=0$, D_i is the same meaning as mendioned above in Eq.(1). Clearly, it is very easy to calculate Eq. (5).

3. Simulation example

In this section, in order to make a further description of this combined method mention above, the hybrid method was applied to the synthesis of ground motions for one dip-slip fault in 3-layer homogeneous half-space.

3.1 Fault model

The fault model is shown in Fig. 4(a), here 20 observation points are located on the free surface along the line perpendicular to the fault; points 1~10 are located on the foot-wall, and points 11~20 are on the hanging-wall side. The points closest to the fault trace with an interval of 100 m are 10 and 11. The material properties of the 3-layered half-space are listed in Table 1, and the fault parameters for the reverse fault are given in Table 2. The rupture velocity is 2.48 km/s. The slip function is assumed as a tringle as schematized in Fig. 4(b). One thing should be noted that, the slip distribution relationship between these two methods should be identical.

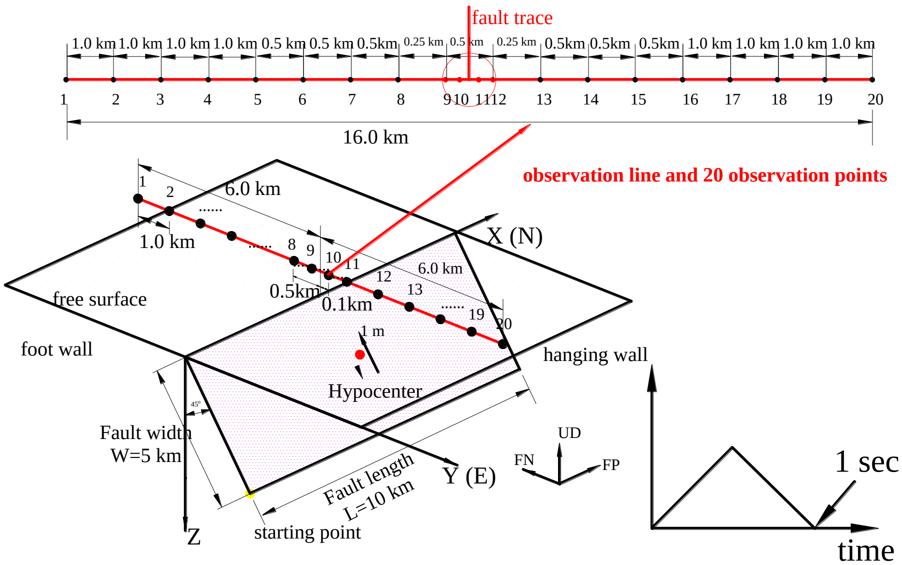

(a) resverse-fault model with surface faulting and observation line(including 20 observation points)

(b) slip velocity

Fig. 4 – Reverse faulting model (with 20 observation points)

Table 1 – Fault parameters

Seismic moment Mo (dyne.cm)		3.825 ×10^{25}
Strike (°)		0
Dip (°)		45
Rake (°)		90
Length (km)		10.0
Width (km)		5.0
Hypocenter (km)	x	5.0
	y	1.77
	z	1.77
Rise time (s)		1.0

Table 2 – Material properties of the layered half-space

Number of the layer	Density (g/cm^3)	V_p (km/s)	V_s (km/s)	Q_p	Q_s	Thickness (km)
1	2200	3.0	1.0	100	50	0.100
2	2400	4.0	2.0	150	75	0.500
3	2500	5.0	3.0	200	100	-

3.2 Simulated results

As for the recordings of near-fault zone, which is typically thought that at a distance about 20 km around the seismic source, the ground motions can exhibit significantly different characteristics than the ones that located further from the seismic sources. An important feature that sometimes occurs in near-fault ground motions is a large pulse in velocity [16]. In addition, due to the permanent ground displacement at the site resulting from tectonic movement, ground motions close to the surface rupture may contain a significant permanent static displacement, which is termed 'fling-step' [17]. Here we listed the time-histories of velocity and displacements along the fault-normal and up-down directions to check the characteristics of near-fault grounds calculated by this method. It should be mentioned that this hybrid method aims at engineering application, a band-pass filter (0.01~20Hz) and a baseline correction have been conducted on the simulated results. Fig.5 (a) ~ (c) and (d) ~ (f) show the results along the fault normal (namely along the EW direction), both including the dynamic terms, static terms, and total components at the 20 observation points, respectively. Fig. 6, (a) ~ (c) listed the velocity time histories, and (d) ~ (f) of displacement time histories along the UD (up-down) direction.

From Figs. 5 (a)~(c) and 6 (a)~(c), an intensive impulsive velocity effect induced from the rupture directivity process can be seen easily. In terms of the fling-step effects, as Figs. 5 (e)~(f) and 6 (e)~(f) showed, the nonzero final displacement occurred at the end of shaking. However, along with the increasing of distance from the fault reaction, the static terms attenuated very fast.

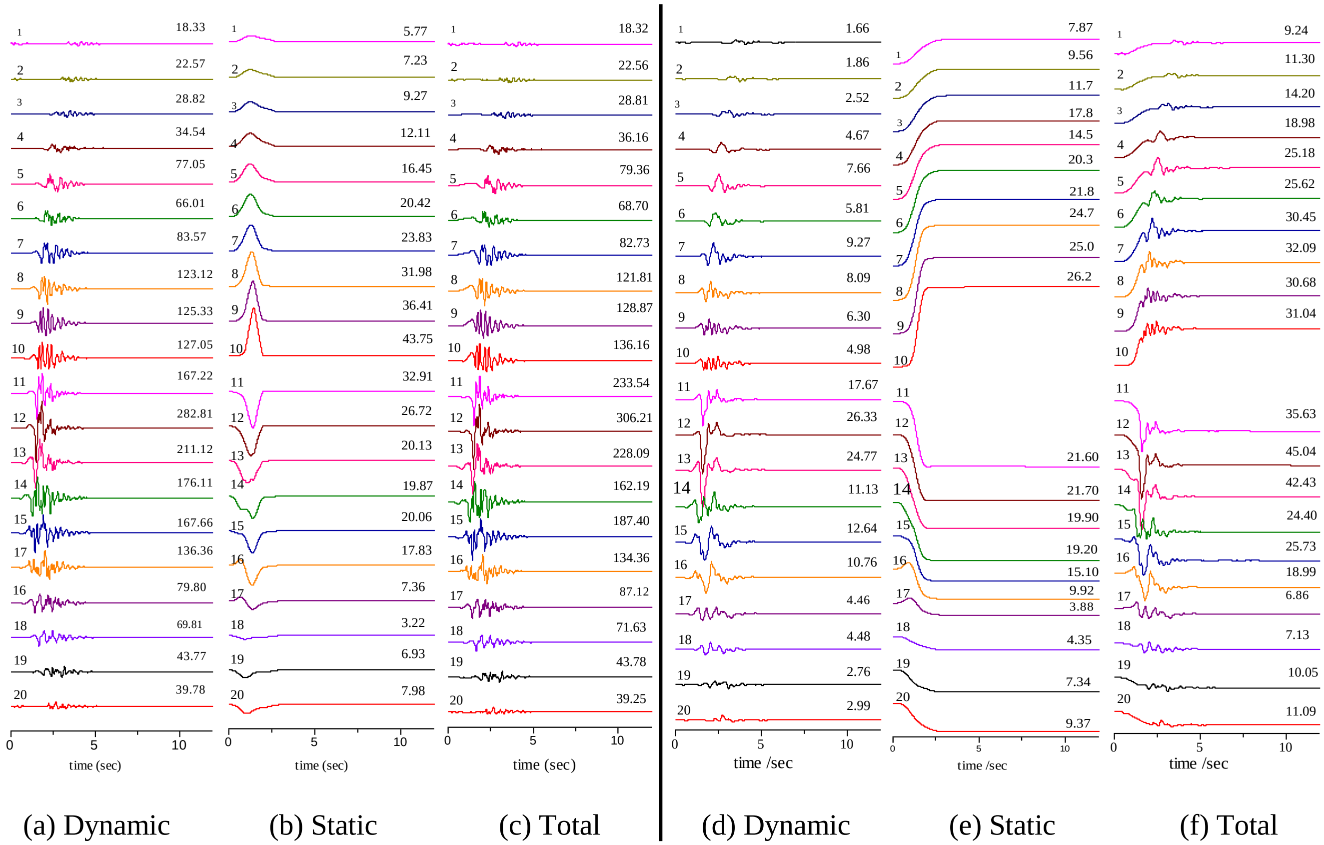

Fig. 5- Time history along EW direction, velocity (a) ~ (c)(unit: cm/s), and displacement (d) ~ (f) (unit: cm), the left number are observation points, and the right side are absolute peak value of relative point)

The simulated results of this reverse-fault also clearly showed the third significant feature of near-fault ground motions: hanging-wall effect. Compared with the footwall (points 1~10), the displacements on hanging wall (points 11~20) have larger values, especially along up-down direction. The main reason for this effect is, as for two points of the same fault-distance on the surface, the hypocenter-distance to the hanging wall point is shorter than the point located in the foot wall, while the attenuation of the fault is rather fast, thus the seismic response of hanging wall sites are much larger than the foot wall sites. Moreover, the multi-reflection and refraction of the propagation waves between the surface ground and the fault planes could contribute to this results.

According to the simulated results and its tendency, this hybrid simulation method can generate the fling-containing time histories which are badly required for the dynamic time-history analysis on structures located near or cross the potential faults.

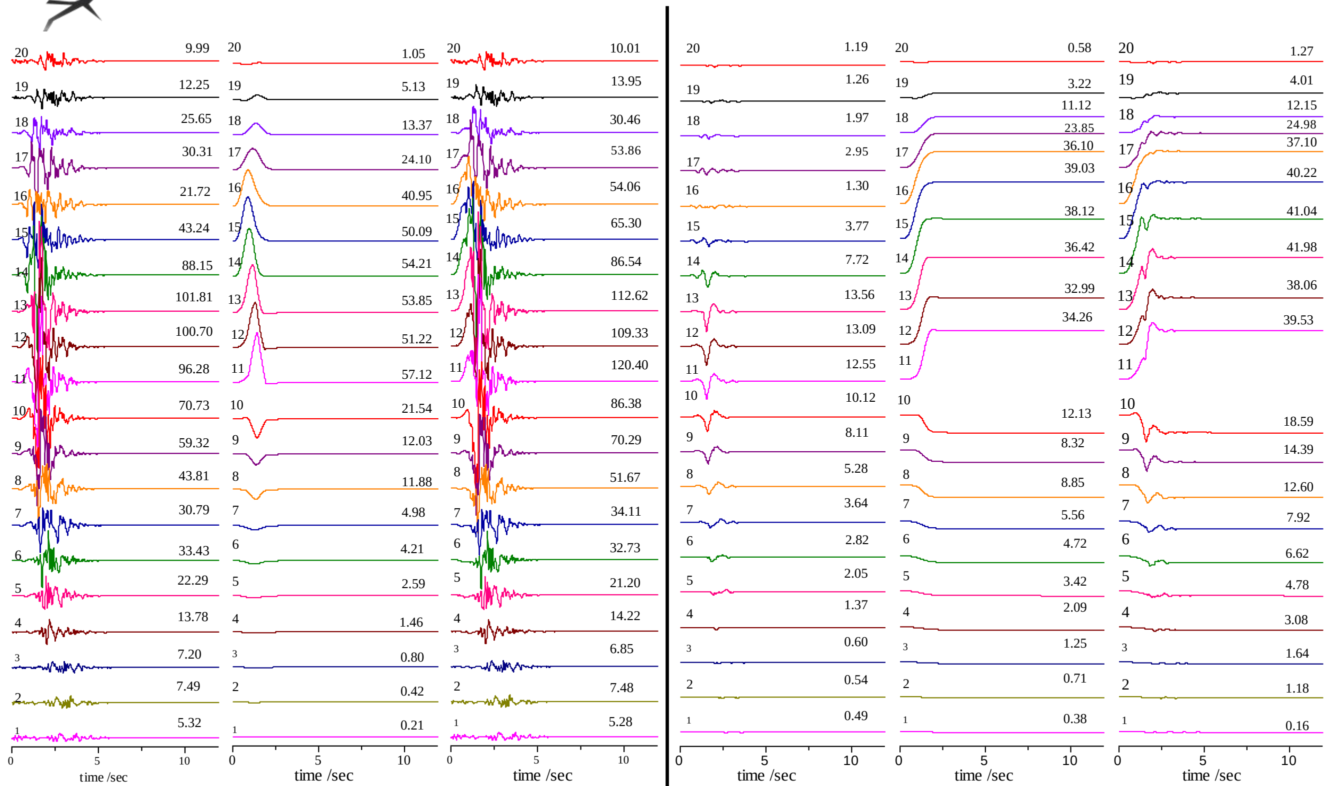

(a) Dynamic (b) Static (c) Total (d) Dynamic (e) Static (f) Total

Fig. 6- Time history along UD direction, velocity (a) ~ (c)(unit: cm/s), and displacement (d) ~ (f) (unit: cm), the left number are observation points, and the right side are absolute peak value of relative point)

4. Seismic response of near-fault bridge structure

As aforementioned, the near-fault ground motions feature much more different from those far-field observed recordings. Whereas significant differences in their respective acceleration-time histories may not be evident, examination of the velocity-time histories and displacement-time histories of these motions reveals the special nature of the pulse-like motion due to forward-directivity effect. The peak value of velocity (PGV) of the near-fault motion is typically substantially greater than that of ordinary strong ground motions, and the loading of the structural system can be affected greatly by this difference [17]. In this paper, the procedure on the seismic analysis of a simplified four-span bridge structure crossing a surface fault subjected to the time-histories of velocity and displacement simulated by the hybrid synthesis method, was presented.

4.1 Bridge model

For the dynamic structures analysis, first, a simplified model of three-degree-of-freedom system and the surface reverse fault(with the same soil situation as in 3.1 above) with its fault plane parameters were proposed as shown in Fig.7. It is assumed that the bridge is 400 m long, it contains four spans and each span is 100 m long. The surface fault is located in middle of the second span. Our main purpose is to check the seismic response of linear behavior of this simplified bridge model under this earthquake. Thus, according to the multi-degree freedom system, we can summarize the motion equations as the matrix formations in Equation (6), which was solved by the Newmark method.

$$[M]\{\ddot{u}\}+[C]\{\dot{u}\}+[K]\{u\}-[D]\{\dot{z}\}-[S]\{z\}=\{0\} \tag{6}$$

where, *[M], [C]* and *[K]* are the mass matrix, the damping matrix and the stiffness matrix of structure, *[D]* and *[S]* are damping matrix and stiffness matrix of spring between the structures and soil. $\{\ddot{u}\}$, $\{\dot{u}\}$ and $\{u\}$ are the response vectors of bridge structure's acceleration, velocity and displacement which under the multi-input velocity and displacement of earthquake ground motion: $\{\dot{z}\}$ and $\{z\}$.

The structural parameters of this bridge structure are listed in Table 3 and Table 4.

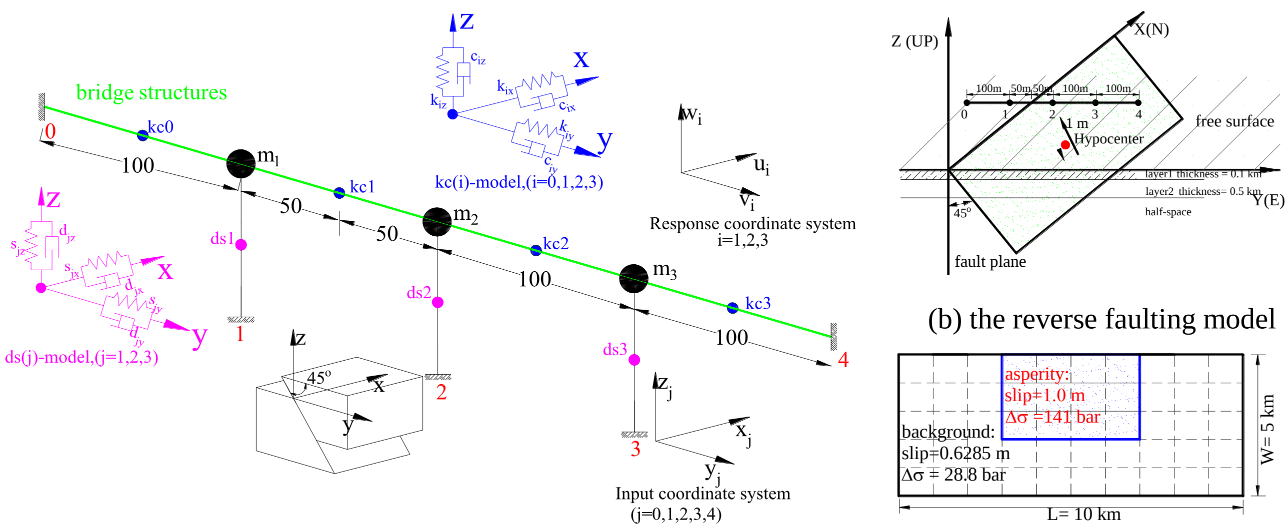

(a) the multi-input bridge model

(b) the reverse faulting model

(c) slip and stress drop

Fig. 7 – Three-dimension bridge model cross a reverse fault

Table 3 – Structural parameters of this system (1)

i	mass 1			mass 2			mass 3		
mass: mi (t/sec^2/m)	0.6			0.4			0.6		
I(1,2or 3)	*x*	*y*	*z*	*x*	*y*	*z*	*x*	*y*	*z*
damping: d_i (t/sec/m)	4	3	5	2	1	3	4	3	5
spring: k_i (t/m)	4000	3000	2000	4000	3000	2000	4000	3000	2000
L: (m)	100			100			100		

Table - 4 Structural parameters of this system (2)

j	0			1			2			3		
	x	*y*	*z*	*x*	*y*	*z*	*x*	*y*	*z*	*x*	*y*	*z*
spring: sj (t/m)	3000	2000	1000	3000	2000	1000	3000	2000	1000	3000	2000	1000
Damping: c_j (t/sec/m))	3	2	1	3	2	1	3	2	1	3	2	1

4.2 Earthquake input

By using the proposed method on near-fault ground motions, the 3-direction velocities (Fig.8) and displacements (Fig. 9) time histories at points 0 to 4 were obtained and used as input motions. All the parameters of the reverse fault, were assumed to be the same as in the calculation above in section 3. The hanging-wall effects (the points 0 and 1 that located on the footwall, gave smaller responses than that at points 2~4 observed on the hanging wall, such as the impulsive velocity and non-zero permanent displacements can be seen obviously.

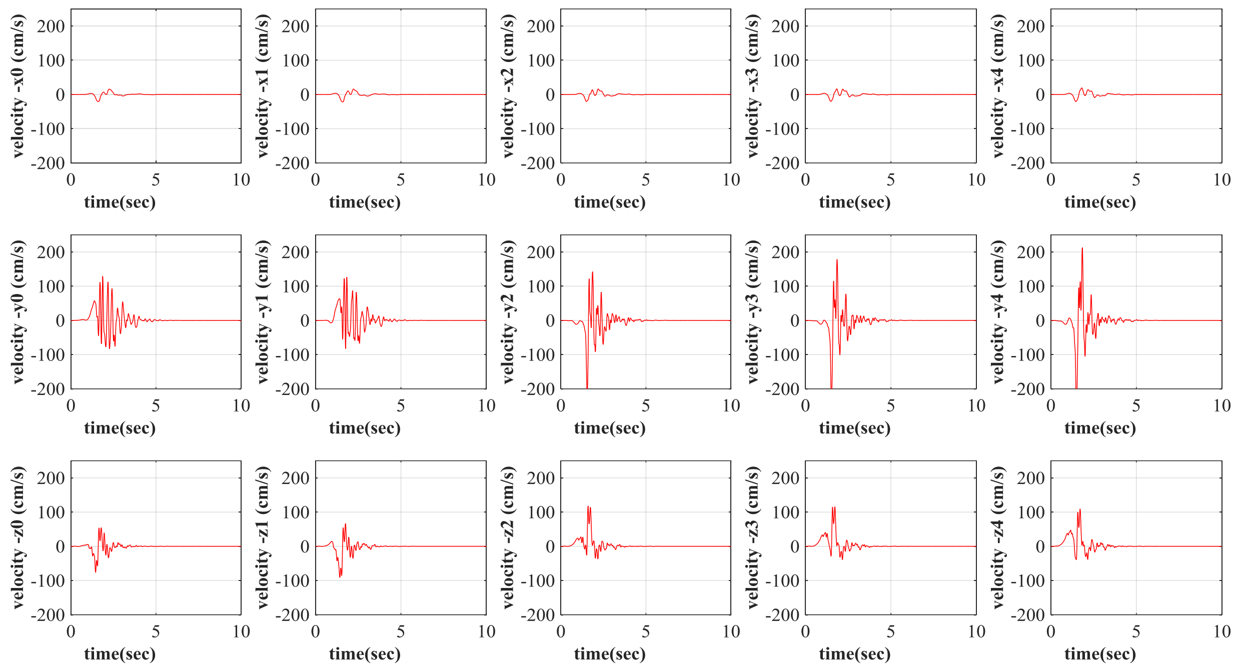

Fig. 8 – Time-history input of velocity

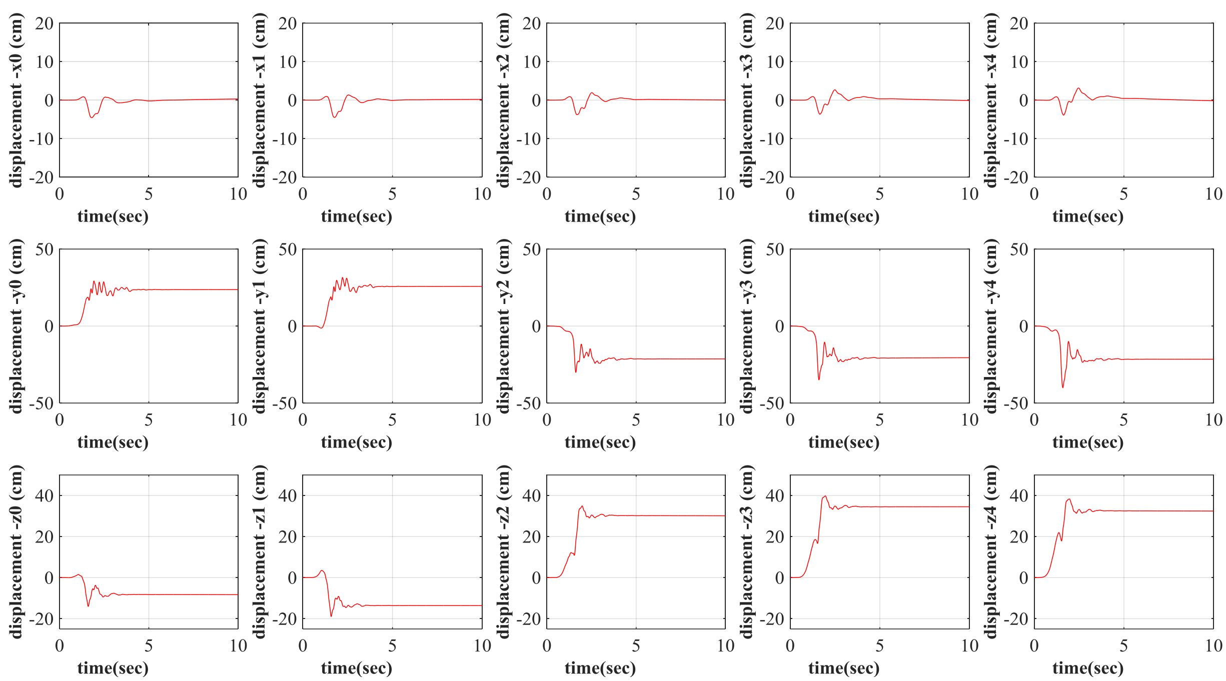

Fig. 9 – Time-history input of displacement

4.3 Response of bridge structures

The seismic structural responses of bridge are shown in Figs. 10~11 for velocity and displacements of each mass, respectively. The asynchronous multi-input ground motions caused large differences in both of velocities and displacement responses, and the velocities show large values under the excitation of static displacement. In addition, the displacements of each mass also results in non-zero values, which should be carefully considered with asynchronous time histories when conducting the seismic analysis or bridge design.

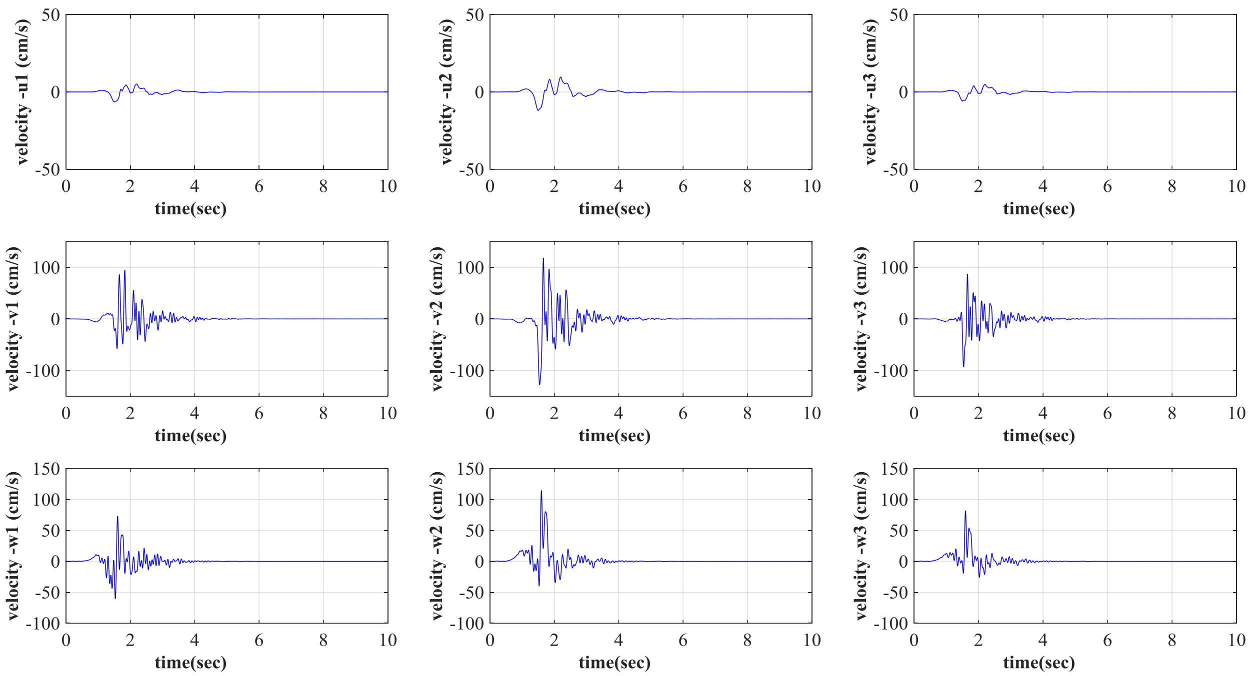

Fig. 10 - The time history of response velocity

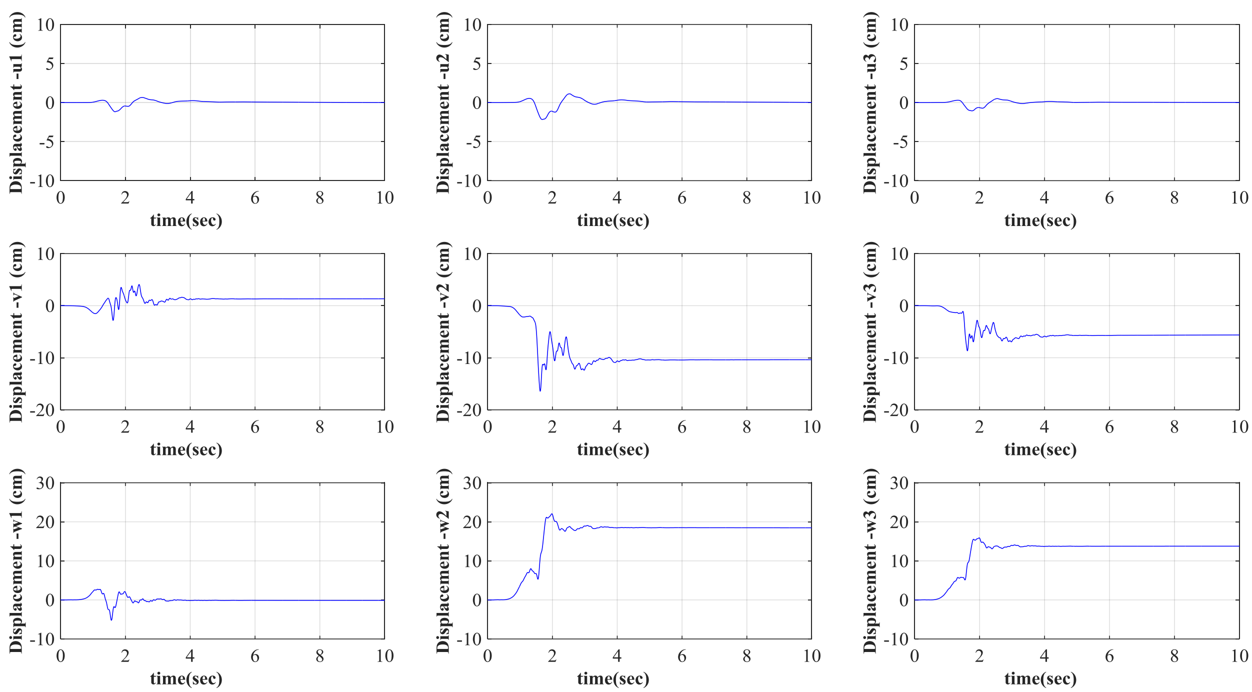

Fig. 11 - The time history of response displacement

5. Discussion

As this proposed method considers only a simple combination of dynamic terms by adoption of stochastic Green's function method and static term of theoretical Green's function method, and linear seismic analysis on a four-spans bridges, some other factors need further research. Firstly, the more realistic situation, e.g., multi-faults, time delay, slip distribution and multi-time windows have to be considered in further studied. Secondly, as for the seismic analysis of bridges, such as different types and its linear and non-linear behavior need further consideration, as well as comparisons with the experiments. Moreover, an exact procedure and synthesis method of ground displacement for bridge design needs further clarifying.

6. Conclusions

(1) A hybrid synthesis method was proposed by combining the modified stochastic Green's function and theoretical Green's function. This hybrid method was developed to simulate the displacement of near-fault strong ground motions, which synthesized both the static and dynamic terms. The simulation results feature the near-fault ground motions characteristics: pulse-like velocity, fling-step displacement and hang-wall effects, which well showed this hybrid simulation method is capable of generating near-fault ground motions.

(2) By applying this method for practical engineering design, the near-fault ground motions were performed to calculated the input velocities and displacements for a simple near-fault bridge model. The strong ground motion demonstrates the near-fault ground motions characteristics: the hanging wall effects, the impulsive effects and non-zero displacement.

(3) The bridge model located near or cross fault exhibits large response values, especially under the input containing impulsive static terms, which should be carefully considered when designing bridge.

Based on the results, the hybrid simulation method of calculating the near-fault displacement (containing the fling-step) for seismic design of such near-fault bridge structures is feasible.

Acknowledgements

Authors referred the program of theoretical Green's function developed by Prof. Hisada, Kogakuin University, which is opened on his web site. Moreover, for the modified stochastic Green's functions, Dr. Nozu, who is from Port and Airport Research Institute, Japan, gave critical and constructive suggestions. This work was supported by Grant-in-Aid for Scientific Research (A) (26249067, principal investigator: Junji Kiyono, Kyoto university).This research also gets support from Do-Yu-Daichi Company. The authors express their gratitude here.

References

[1] Mavroeidis GP, Papageorgiou AS (2003): A mathematical representation of near-fault ground motions, *Bulletin of the Seismological Society of America*, **93**, 1099–1131.

[2] Hongze W (2005): Theoretical method for characterization of near-fault wave motion and response of extended structures, doctoral thesis, University of Miyazaki.

[3] Kojima K, Fujita K, and Takewaki I (2015a). Critical double impulse input and bound of earthquake input energy to building structure. *Front. Built Environ*. 1:5. doi:10.3389/fbuil.2015.00005.

[4] Kojima K, Takewaki I. (2015b). Critical earthquake response of elastic-plastic structures under near-fault ground motions (Part 1: Fling-step input). *Front. Built Environ*. 1:12. doi:10.3389/fbuil.2015.00012.

[5] Kojima K, and Takewaki I (2015b). Critical earthquake response of elastic-plastic structures under near-fault ground motions (part 2: forward-directivity input). Front. Built Environ. 1:13. doi:10.3389/fbuil.2015.00013.

[6] Hisada Y, Bielak J (2003): A theoretical method for computing near-fault strong motions in layered half-space considering static offset due to surface faulting, with a physical interpretation of fling step and rupture directivity, *Bulletin of the Seismological Society of America*, **93**, 1154-1168.

[7] Irikura K (1983): Semi-empirical estimation of strong ground motion during large earthquakes, *Bulletin of the Disaster Prevention Research Institute,* **33**, 63-104.

[8] Irikura K, Miyake H: Lecture Note on strong motion seismology, *http://kojiro-irikura.jp/pdf/Workshop_irikura.pdf.*

[9] Douglas D, Gabriel H, Anil KC, Shawn L (2007): Near-fault seismic ground motions, Report NO. EERC. 2007-03, Earthquake engineering research center, college of engineering university of California, Berkeley.

[10] Onishi Y, Horike M (2004): The extended stochastic simulation method for close-fault earthquake motion prediction and comments for its application to the hybrid method. *Journal of Structural and Construction Engineering,* AIJ 586:37–44. (in Japanese)

[11] Nozu A (2006): A simple scheme to introduce near-field and intermediate-field terms in stochastic Green's function, *Proceedings of 12th Japan Earthquake Engineering Symposium*, 190-193. (in Japanese)

[12] Hisada Y (1994): An efficient method for computing Green's functions for layered half-space with sources and receivers at close depths, *Bulletin of the Seismological Society of America***, 84**(5), 1456-1492.

[13] Hisada Y (1995): An efficient method for computing Green's functions for layered half-space with sources and receivers at close depths (part 2), *Bulletin of the Seismological Society of America,***85**(4), 1080-1093.

[14] Hisada Y (1997): Efficient methods for computing Green's function and normal modes solutions for layered half-spaces, *Journal of Structural and Construction Engineering,AIJ,***501**,49-56. (in Japanese).

[15] Hisada Y, Bielak J (2002): An analytical method for simulating near source strong ground motion considering permanent displacement due to fault slip, *the 11st Japan Earthquake Engineering Symposium*, 167-172. (in Japanese)

[16] Abrahamson NA (2002): Velocity pulses in near-fault ground motions, *in Proceedings of the UC Berkeley—CUREE Symposium in Honor of Ray Clough and Joseph Penzien: Berkeley, California*, UC Berkeley, Consortium of Universities for Research in Earthquake Engineering, 9–11 May 2002, 40–41.

[17] Jonatha DB, Adrian RM (2004): Characterization of forward-directivity ground motions in the near-fault region, *Soil dynamics and earthquake engineering***, 24**: 815-828.